Original paper

The mathematical characteristic of the fifth order Laplace contour filters used in digital image processing

Ireneusz Winnicki*, Slawomir Pietrek, Janusz Jasinski, Krzysztof Kroszczynski

Military University of Technology, Warsaw, Poland

e-mail: ireneusz.winnicki@wat.edu.pl; ORCID: http://orcid.org/0000-0001-9170-422X
e-mail: slawomir.pietrek@wat.edu.pl; ORCID: http://orcid.org/0000-0001-9890-8487
e-mail: janusz.jasinski@wat.edu.pl; ORCID: http://orcid.org/0000-0001-5634-3430
e-mail: krzysztof.kroszczynski@wat.edu.pl; ORCID: http://orcid.org/0000-0003-1197-9915

*Corresponding author: Ireneusz Winnicki, e-mail: ireneusz.winnicki@wat.edu.pl

Abstract: The Laplace operator is a differential operator which is used to detect edges of objects in digital images. This paper presents the properties of the most commonly used fifth-order pixels Laplace filters including the difference schemes used to derive them (finite difference method – FDM and finite element method – FEM). The results of the research concerning third-order pixels matrices of the convolution Laplace filters used for digital processing of images were presented in our previous paper: The mathematical characteristic of the Laplace contour filters used in digital image processing. The third order filters is presented by Winnicki et al. (2022). As previously, the authors focused on the mathematical properties of the Laplace filters: their transfer functions and modified differential equations (MDE). The relations between the transfer function for the differential Laplace operator and its difference operators are described and presented here in graphical form. The impact of the corner elements of the masks on the results is also discussed. A transfer function, is a function characterizing properties of the difference schemes applied to approximate differential operators. Since they are relations derived in both types of spaces (continuous and discrete), comparing them facilitates the assessment of the applied approximation method.

1. Introduction

The difference methods started to develop intensively in the middle of 1940s. At that time every new proposal of a difference scheme for the differential operator of the first

and second order was applied mainly to numerical weather prediction. In early 1950s the scientists from the Joint Numerical Weather Prediction Unit (U.S. Air Force): Knighting (1955), Thompson (1955a, b) and Shuman (1956), presented proposals of nine, thirteen and twenty-five-point difference schemes on square 5×5 pixels stencils – see: Ogura (1958), Miyakoda (1960) and Gates (1961).

In this paper, using matrices induced by difference schemes approximating the Laplace operator, the authors: derived the Π-forms of the first differential approximation of the schemes (modified differential equations); determined the transfer functions of the $f_p(\widetilde{k}, \widetilde{l})$ (where p is the matrix number explained in the paper body; $\widetilde{k} = kh/\pi$ and $\widetilde{l} = lh/\pi$ – the Nyquist wave-numbers which are the wave-numbers normalized to the maximum wave-number that can be sampled and k, l – wave-numbers, $k = 2\pi/\lambda_x$, $l = 2\pi/\lambda_y$, and λ_x and λ_y – the wavelengths); presented graphical interpretation of these functions as well as the relation between the transfer function of $f_p(\widetilde{k}, \widetilde{l})$ and $f_L(\widetilde{k}, \widetilde{l})$ for the differential Laplace operator, i.e. the $f_p(\widetilde{k}, \widetilde{l})/f_L(\widetilde{k}, \widetilde{l})$ relation.

A transfer function, is a function characterizing properties of the difference schemes applied to approximate differential operators. Since they are relations derived in both types of spaces (continuous and discrete), comparing them facilitates the assessment of the applied approximation method. Therefore, the transfer operator presents spectral properties of matrices of linear convolution filters as functions of the $\widetilde{k}$ and $\widetilde{l}$ Nyquist wave-numbers. The values of $f_p(\widetilde{k}, \widetilde{l})$ and $f_L(\widetilde{k}, \widetilde{l})$ are indirectly generated by the lengths of the disturbances occurring during analyses of the digital fields. More details are available in Pitas (2000), Jähne (2002), Strikwerda (2004), Burger and Burge (2008), Burger and Burge (2009a, b), Iserles (2009), Mallat (2009), Parker (2011), Petrou and Petrou (2011), Gonzalez and Woods (2018). The course studies of the $f_p(\widetilde{k}, \widetilde{l})$ functions will be used for presenting the properties of the specific Laplace filters. The comparison will be conducted over a test field created in the Matlab by means of the *peaks.m* script.

The fifth-order 5×5 pixels Laplace filters matrices consideration from the point of view of numerical methods is an important aspect of the discussion presented here. Each matrix constitutes other difference scheme applicable to computational methods. It is a different method of obtaining approximate solutions of second order differential equations in which the ∇^2 operator occurs – see: Prewitt (1970), Jähne et al. (1999), Pitas (2000), Scharr (2000), Scharr and Weickert (2000), Jähne (2002), Pratt (2007), Burger and Burge (2008), Burger and Burge (2009a, b), Mallat (2009), Parker (2011), Petrou and Petrou (2011), Krawczyk et al. (2012), Gonzalez and Woods (2018). The properties of the analyzed matrices should be taken into account when solving selected issues of the mathematical physics.

The paper presents the descriptions of seven selected masks of the Laplace type used in the processing and interpretation of digital data of various origin. As we have already mentioned in Winnicki et al. (2022) this may be navigation data (Borawski, 2004; Stateczny and Nowakowski, 2006; Burger and Burge, 2009a; Stateczny et al., 2021) radar, sonar and satellite (Kurczynski et al., 2017; Fryskowska et al., 2019; Stateczny et al., 2020), geodetic and cartographic (called remotely sensed in Kupidura and Kupidura (2009), Kupidura et al. (2010)), meteorological (Jasinski et al. (1999) – information

about clouds including its shape, size, internal structure, as well as the relationship of the location of different types of clouds). These may also be digital images of building infrastructure elements (Burger and Burge, 2009a; Reda and Kedzierski, 2020; Wojtkowska et al., 2021) and technical devices (Pokonieczny and Moscicka, 2018). A common goal appears in each of the listed here areas of photogrammetric research: correct edge and vertex detection of the analyzed objects.

The contextual filter is primarily a multi-element mask described by an odd order square matrix. For this reason, the final forms of most of the used fifth-order Laplace filter masks together with their Π-forms of the first differential approximation are derived here. In Section 2 we discuss the origin of some filter masks built on the basis of the finite difference method (FDM) and of the finite element method (FEM). In Section 3 we discuss the numerical test and in Section 4 the final conclusions are presented. The authors also want to highlight the development of the difference scheme for the differential Laplace operator built on the 5×5 pixels square grid. In Part I (Winnicki et al., 2022), we presented the spectral characteristic of the third order filters of the Laplace type.

2. The difference Laplace filters of the fifth order

Laplace filter masks are induced by the two-dimensional difference operator for the partial differential equation (PDE):

$$\mathbb{A}u = \Delta u = \nabla^2 u = \frac{\partial^2 u}{\partial x^2} + \frac{\partial^2 u}{\partial y^2}, \tag{1}$$

where: $u(x, y)$ – any scalar function. Assuming that the solution of (1) may be presented as an individual Fourier mode:

$$u(x_m, y_n) = u_{m,n} = \hat{u} e^{i(\widetilde{k} x_m + \widetilde{l} y_n)}. \tag{2}$$

We obtain the transfer function for the Laplace equation (1):

$$\nabla^2 u_{m,n} = -\pi^2 \left(\widetilde{k}^2 + \widetilde{l}^2 \right) \hat{u} e^{i\pi(\widetilde{k} x_m + \widetilde{l} y_n)} = f_L(\widetilde{k}, \widetilde{l})_L u_{m,n} \tag{3}$$

depends on the Nyquist wave-numbers $(\widetilde{k}, \widetilde{l})$; $f_L(\widetilde{k}, \widetilde{l}) = -\pi^2(\widetilde{k}^2 + \widetilde{l}^2)$ – transfer function for the Laplace operator (see Fig. 1). We can also call it the transfer function of the derived filter (see Jähne (2002)).

The forms of the Laplace masks depend on the method of discretization of the differential operator (1). The finite difference method and the finite element method are commonly applied in practice. The finite difference discretization of operator $\mathbb{A}$ (in the former method) and the approximation of the solution (in the latter) are provided on the mesh of equidistant grid nodes.

In the FEM the sought after solution $u(x, y)$ in $\mathbb{A}u$ is approximated by the following series:
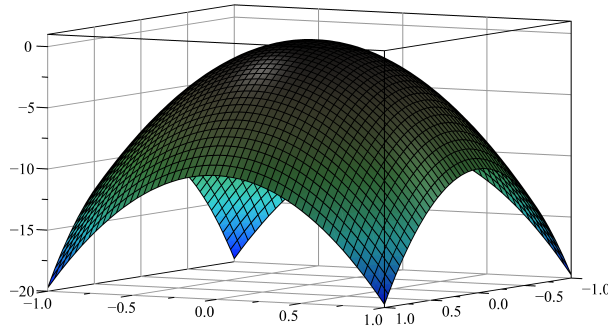
$$u(x, y) = \sum_{i,j} u_{i,j} \varphi_i(x) \psi_j(y), \tag{4}$$

Fig. 1. The transfer function $f_L(\widetilde{k}, \widetilde{l})$ for the differential Laplace equation – negative
in the range of $(\widetilde{k}, \widetilde{l}) = [-1 \div 1] \times [-1 \div 1]$

where: $u_{i,j}$ values of the function $u(x, y)$ in the grid nodes (i, j); $\varphi_i(x)$, $\psi_j(y)$ basic functions of one variable, often called the Lagrange elements. In this paper these functions are the polynomials of the second degree (parabolas).

In most cases the discussed difference schemes are different although they approximate the same differential operator. They differ in the forms – in the case of FEM they strictly depend on the basic functions degree (see Subsection 2.2) – and they have different characteristics. In both cases, sets of the multi-point filters in the form of 5×5 pixels matrices are obtained.

The forms of the MDEs are very useful in the detailed analysis of the dispersive and dissipative features of the difference schemes (see: Appadu et al. (2008), Appadu and Dauhoo (2011), Appadu (2014)). For the elliptic partial differential equations we always obtain their Π-forms. More work on the MDE can be found in Warming and Hyett (1974), Peyret and Taylor (1983), Li and Yang (2011), Winnicki et al. (2019), Shokin et al. (2020a, b).

2.1. The difference Laplace filters of the fifth order

Let us start the discussion on the influence of the Laplace difference scheme form on the accuracy of various numerical solutions from the fifth-order Laplacian presented and discussed by: Knighting (1955), Thompson (1955a, b), Ogura (1958), Miyakoda (1960) and Torre and Poggio (1984). It is the classical sum of the fourth-order finite difference equation (FDE) with respect to x and y:

$$\mathbb{A}_1^5 u_h = \frac{16(u_{i-1,j} + u_{i,j+1} + u_{i+1,j} + u_{i,j-1})}{12h^2}$$
$$- \frac{60u_{i,j} + u_{i-2,j} + u_{i,j+2} + u_{i+2,j} + u_{i,j-2}}{12h^2}, \tag{5}$$

which leads to the Laplace filter mask (u_h – the approximated solution, h – spatial step of the regular square mesh, in this case – the distance between pixels). It is always assumed

that $h_x = h_y = h = 1$ in both directions of x and y. Therefore the filter mask can be written in the following form:

$$\mathbf{Lap}_1^5 = \frac{1}{12} \begin{bmatrix} 0 & 0 & -1 & 0 & 0 \\ 0 & 0 & 16 & 0 & 0 \\ -1 & 16 & -60 & 16 & -1 \\ 0 & 0 & 16 & 0 & 0 \\ 0 & 0 & -1 & 0 & 0 \end{bmatrix}. \tag{6}$$

Equation (5) is the first commonly used in numerical weather prediction nine-point FDE based on the "cross" 25-point stencil with 9 non-zero coefficients. In our opinion, (6) should be recognized as the first 5×5 pixels filter mask of the Laplace type applied in the digital image processing. The remaining 16 coefficients in the mask (6) are equal to zero and they are ignored in the computations. The MDE for (5) is presented below:

$$\Pi_1^5 = \nabla^2 u - \frac{h^4}{90} \left(\frac{\partial^6 u}{\partial x^6} + \frac{\partial^6 u}{\partial y^6} \right) - \frac{h^6}{1008} \left(\frac{\partial^8 u}{\partial x^8} + \frac{\partial^8 u}{\partial y^8} \right) + O(h^8). \tag{7}$$

In equation (7), we have only the unmixed even-order partial derivatives. The mixed derivatives are associated with the coefficients lying outside the "cross" (see for example equation (11) and the next masks).

In Winnicki et al. (2022) three terms were defined: convergence, order of accuracy and consistency with reference to the difference scheme and to the MDE. We do not repeat them here. However, as $h \to 0$ equation (7) approaches $\nabla^2 u = \dfrac{\partial^2 u}{\partial x^2} + \dfrac{\partial^2 u}{\partial y^2}$. So the FDE (5) is a consistent approximation of the Laplace equation and its solution $u_h(x_i, y_j)$ converges to the exact solution $u(x, y)$. The accuracy of the difference equation (5) is of the fourth order. However, according to the spectral theory the coefficient in front of the sum $\left(\dfrac{\partial^8 u}{\partial x^8} + \dfrac{\partial^8 u}{\partial y^8} \right)$ should be equal to $+h^6/1008$ (we marked in red all the terms of the modified differential equations and transfer functions in Taylor expansion which coefficients have incorrect signs – it is, of course, the feature of the FDEs and, consequently, of the filter masks and their MDEs).

The transfer function for (5) has the form:

$$f_1^5(\widetilde{k}, \widetilde{l}) = \frac{-64 \sin^2 \dfrac{\pi \widetilde{k}}{2} - 64 \sin^2 \dfrac{\pi \widetilde{l}}{2} + 4 \sin^2(\pi \widetilde{k}) + 4 \sin^2(\pi \widetilde{l})}{12}. \tag{8}$$

The Taylor expansion of (8) for the Nyquist wave-numbers $\widetilde{k}$ and $\widetilde{l}$ up to the eighth order yields the approximation:

$$f_{1T}^5(\widetilde{k}, \widetilde{l}) = -\pi^2 \left(\widetilde{k}^2 + \widetilde{l}^2 \right) - \frac{\pi^6}{90} \left(\widetilde{k}^6 + \widetilde{l}^6 \right) - \frac{\pi^8}{1008} \left(\widetilde{k}^8 + \widetilde{l}^8 \right) + O(\widetilde{k}^{10}, \widetilde{l}^{10}). \tag{9}$$

Figure 2 is a graphical presentation of the transfer function (8) for the difference scheme (5) (Fig. 2a) and for the relation $\dfrac{f_1^5(\widetilde{k},\widetilde{l})}{f_L(\widetilde{k},\widetilde{l})}$ (Fig. 2b). Thompson (1955b) (see also: Miyakoda (1960), p. 97 and Ogura (1958), p. 477) proposed another difference scheme for the discretization of the operator (1):

$$
\begin{aligned}
A_2^5 u_h = {}& \frac{24(u_{i-1,j} + u_{i,j+1} + u_{i+1,j} + u_{i,j-1}) - 84u_{i,j}}{16h^2} \\
& - \frac{u_{i-2,j} + u_{i,j+2} + u_{i+2,j} + u_{i,j-2}}{16h^2} \\
& - \frac{2(u_{i-1,j+1} + u_{i+1,j+1} + u_{i+1,j-1} + u_{i-1,j-1})}{16h^2},
\end{aligned} \tag{10}
$$

which also leads to the 5×5 pixels filter mask of the Laplace type:

$$
\mathbf{Lap}_2^5 = \frac{1}{16}
\begin{bmatrix}
0 & 0 & -1 & 0 & 0 \\
0 & -2 & 24 & -2 & 0 \\
-1 & 24 & -84 & 24 & -1 \\
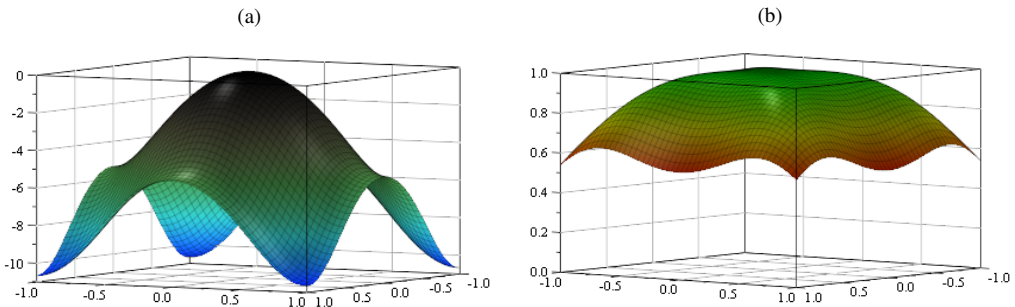0 & -2 & 24 & -2 & 0 \\
0 & 0 & -1 & 0 & 0
\end{bmatrix}. \tag{11}
$$

(a)   (b)

Fig. 2. The transfer function $f_1^5(\widetilde{k},\widetilde{l})$ for the mask (6) – negative in the entire range of $(\widetilde{k},\widetilde{l})$ (a)

and the graph of $\dfrac{f_1^5(\widetilde{k},\widetilde{l})}{f_L(\widetilde{k},\widetilde{l})}$ (b)

The MDE for the difference scheme (10) has the form:

$$
\begin{aligned}
\Pi_2^5 = {}& \nabla^2 u + \frac{h^2}{48}\left(\frac{\partial^4 u}{\partial x^4} + \frac{\partial^4 u}{\partial y^4}\right) - \frac{h^2}{8}\frac{\partial^4 u}{\partial x^2 \partial y^2} + \frac{11h^4}{1440}\left(\frac{\partial^6 u}{\partial x^6} + \frac{\partial^6 u}{\partial y^6}\right) \\
& - \frac{h^4}{96}\left(\frac{\partial^6 u}{\partial x^4 \partial y^2} + \frac{\partial^6 u}{\partial x^2 \partial y^4}\right) - \frac{h^6}{1152}\frac{\partial^8 u}{\partial x^4 \partial y^4} - \frac{59h^6}{80640}\left(\frac{\partial^8 u}{\partial x^8} + \frac{\partial^8 u}{\partial y^8}\right) + O(h^8).
\end{aligned} \tag{12}
$$

The transfer functions for the scheme (10) are as follows (Fig. 3a):

$$f_2^5(\widetilde{k},\widetilde{l}) = -5\sin^2\frac{\pi\widetilde{k}}{2} - 5\sin^2\frac{\pi\widetilde{l}}{2} - 2\sin^2\frac{\pi\widetilde{k}}{2}\sin^2\frac{\pi\widetilde{l}}{2} + \frac{\sin^2\pi\widetilde{k} + \sin^2\pi\widetilde{l}}{4}, \qquad (13)$$

$$f_{2T}^5(\widetilde{k},\widetilde{l}) = -\pi^2\left(\widetilde{k}^2 + \widetilde{l}^2\right) + \frac{\pi^4}{48}\left(\widetilde{k}^4 + \widetilde{l}^4\right) - \frac{\pi^4}{8}\widetilde{k}^2\widetilde{l}^2 + \frac{11\pi^6}{1440}\left(\widetilde{k}^6 + \widetilde{l}^6\right)$$
$$- \frac{\pi^6}{96}\left(\widetilde{k}^4\widetilde{l}^2 + \widetilde{k}^2\widetilde{l}^4\right) - \frac{\pi^8}{1152}\widetilde{k}^4\widetilde{l}^4 - \frac{59\pi^8}{80640}\left(\widetilde{k}^8 + \widetilde{l}^8\right) + O(\widetilde{k}^{10},\widetilde{l}^{10}). \quad (14)$$

The mixed partial derivatives in (12) and the products of $\widetilde{k}$ and $\widetilde{l}$ in (14) are the consequence of the non-zero elements (here equal to -2) that appeared in the corners of the nine-point square stencil in the red boxes of the matrix (11). The sum: $-\dfrac{h^2}{8}\dfrac{\partial^4 u}{\partial x^2 \partial y^2} +$

$\dfrac{11h^4}{1440}\left(\dfrac{\partial^6 u}{\partial x^6} + \dfrac{\partial^6 u}{\partial y^6}\right) - \dfrac{h^6}{1152}\dfrac{\partial^8 u}{\partial x^4 \partial y^4} - \dfrac{59h^6}{80640}\left(\dfrac{\partial^8 u}{\partial x^8} + \dfrac{\partial^8 u}{\partial y^8}\right)$ in (12) describes the effects of anti-dissipation (see Shokin et al. (2020b)), also called backward diffusion. It follows the exponential growth of the amplitude of the elementary solution and presents the amplification features of this scheme.
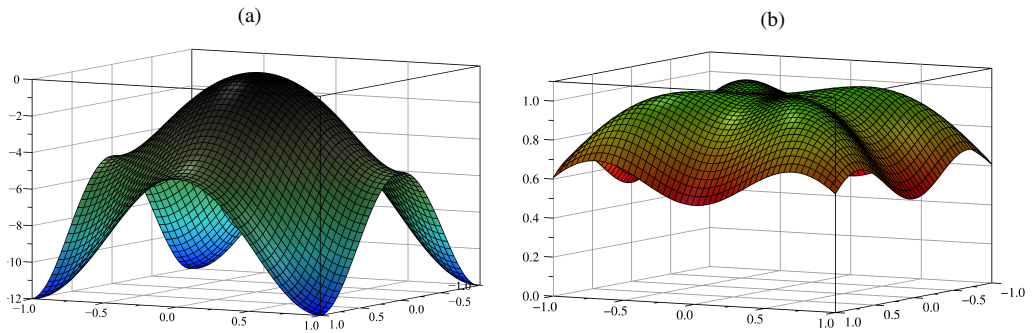

Fig. 3. The transfer function $f_2^5(\widetilde{k},\widetilde{l})$ for the mask (11) – negative in the entire range of $(\widetilde{k},\widetilde{l})$ (a) and the graph of $\dfrac{f_2^5(\widetilde{k},\widetilde{l})}{f_L(\widetilde{k},\widetilde{l})}$ (b)

Despite these features, FDE (10) is consistent and convergent as $h \rightarrow 0$ and its accuracy is of the second order. For medium values of the Nyquist wave-numbers the relation $f_2^5(\widetilde{k},\widetilde{l})/f_L(\widetilde{k},\widetilde{l})$ exceeds 1 (Fig. 3b and Fig. 4).

Comparing Figure 2b and Figure 3b we conclude that, although the accuracy of the filter (11) is of the second order, its conformity to the transfer function of the Laplace operator for the large Nyquist wave-numbers is better than of the mask (6) with the accuracy of the fourth order.
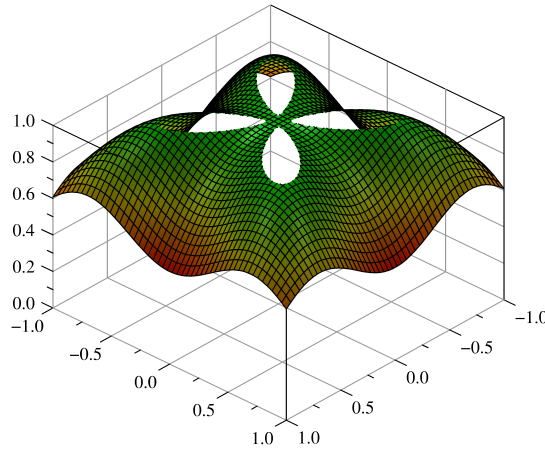
Fig. 4. The graph of $\dfrac{f_2^5(\widetilde{k}, \widetilde{l})}{f_L(\widetilde{k}, \widetilde{l})}$. The white areas in the shape of teardrops indicate the areas

where the function $\dfrac{f_2^5(\widetilde{k}, \widetilde{l})}{f_L(\widetilde{k}, \widetilde{l})}$ exceeds 1

The accuracy of the next difference scheme for the Laplace operator (1) proposed by Gates (1956) (see Burger and Burge, 2009a, 2009b):

$$
\begin{aligned}
\mathbb{A}_3^5 u_h = & -\frac{u_{i-2,j} + u_{i,j+2} + u_{i+2,j} + u_{i,j-2}}{36h^2} - \frac{60u_{i,j}}{36h^2} \\
& - \frac{14(u_{i-1,j} + u_{i,j+1} + u_{i+1,j} + u_{i,j-1})}{36h^2} \\
& + \frac{32(u_{i-1,j+1} + u_{i+1,j+1} + u_{i-1,j-1} + u_{i+1,j-1})}{36h^2} \\
& - \frac{u_{i-2,j+1} + u_{i+2,j+1} + u_{i-2,j-1} + u_{i+2,j-1}}{36h^2} \\
& - \frac{u_{i-1,j+2} + u_{i+1,j+2} + u_{i-1,j-2} + u_{i+1,j-2}}{36h^2}
\end{aligned}
\tag{15}
$$

is of the second order. This scheme leads to the filter mask:

$$
\mathbf{Lap}_3^5 = \frac{1}{36}
\begin{bmatrix}
0 & -1 & -1 & -1 & 0 \\
-1 & 32 & -14 & 32 & -1 \\
-1 & -14 & -60 & -14 & -1 \\
-1 & 32 & -14 & 32 & -1 \\
0 & -1 & -1 & -1 & 0
\end{bmatrix}.
\tag{16}
$$

The construction of the filter (16) is rather simple. The approximation of the accuracy of the fourth order for one term of the Laplace operator is: $\dfrac{\partial^2 u}{\partial x^2} \rightarrow \begin{bmatrix} -1 & 16 & -30 & 16 & -1 \end{bmatrix}$

and the same for $\dfrac{\partial^2 u}{\partial y^2}$ (see (6)). The 5×5 pixels matrix (16) is the sum of the two 5×5 matrices with the same three rows and three columns:

$$
\frac{1}{36}
\begin{bmatrix}
0 & 0 & 0 & 0 & 0 \\
-1 & 16 & -30 & 16 & -1 \\
-1 & 16 & -30 & 16 & -1 \\
-1 & 16 & -30 & 16 & -1 \\
0 & 0 & 0 & 0 & 0
\end{bmatrix}
+
\frac{1}{36}
\begin{bmatrix}
0 & -1 & -1 & -1 & 0 \\
0 & 16 & 16 & 16 & 0 \\
0 & -30 & -30 & -30 & 0 \\
0 & 16 & 16 & 16 & 0 \\
0 & -1 & -1 & -1 & 0
\end{bmatrix}
$$

$$
=
\frac{1}{36}
\begin{bmatrix}
0 & -1 & -1 & -1 & 0 \\
-1 & 32 & -14 & 32 & -1 \\
-1 & -14 & -60 & -14 & -1 \\
-1 & 32 & -14 & 32 & -1 \\
0 & -1 & -1 & -1 & 0
\end{bmatrix}.
\tag{17}
$$

In Gates (1961) the value of the coefficient in (16) is equal to $\dfrac{1}{24}$. After detailed analysis of the MDE for (15) (see (18)) we conclude that it is incorrect, and its correct value is $1/36$.

This modification of the filter mask (6) did not improve its spectral features. Analyzing Fig. 5b one can say that the spectral features of (16) are evidently worse than those of (6), especially for medium and large Nyquist wave-numbers.
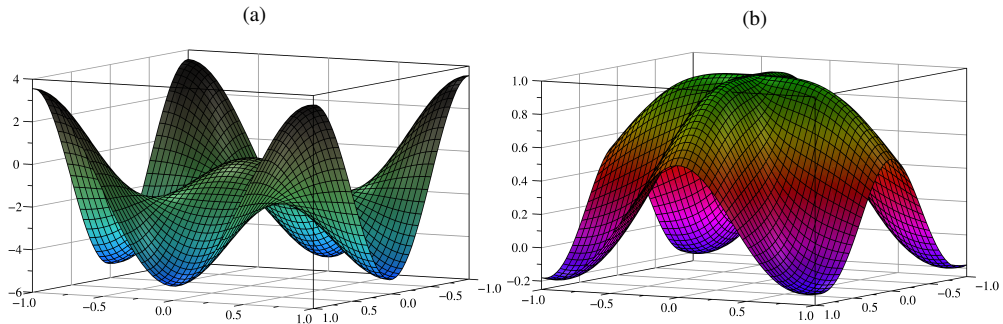
(a) (b)

Fig. 5. The function $f_3^5(\widetilde{k}, \widetilde{l})$ for the mask (16) – negative for small and medium wave-numbers $(\widetilde{k}, \widetilde{l})$ (a) and the graph of $\dfrac{f_3^5(\widetilde{k}, \widetilde{l})}{f_L(\widetilde{k}, \widetilde{l})}$ (b)

The FDE (15) is a consistent approximation of the Laplace equation and if $h \to 0$ its solution $u_h(x_i, y_j)$ converges to the exact solution $u(x, y)$. The MDE for the difference scheme (15) has the form:

$$
\Pi_3^5 = \nabla^2 u + \frac{2h^2}{3} \frac{\partial^4 u}{\partial x^2 \partial y^2} + \frac{h^4}{90} \left(\frac{\partial^6 u}{\partial x^6} + \frac{\partial^6 u}{\partial y^6} \right) - \frac{h^6}{1008} \left(\frac{\partial^8 u}{\partial x^8} + \frac{\partial^8 u}{\partial y^8} \right)
$$

$$
- \frac{h^4}{36} \left(\frac{\partial^6 u}{\partial x^4 \partial y^2} + \frac{\partial^6 u}{\partial x^2 \partial y^4} \right) + O(h^8).
\tag{18}
$$

In (18) we can also find the mixed even-order partial derivatives. However, for large Nyquist wave-numbers $(\widetilde{k}, \widetilde{l})$, $|\widetilde{k}| \to 1$ and $|\widetilde{l}| \to 1$ the transfer function $f_3^5(\widetilde{k}, \widetilde{l})$ rapidly grows and achieves values nearly 4 while the relation $f_3^5(\widetilde{k}, \widetilde{l})/f_L(\widetilde{k}, \widetilde{l})$ rapidly decreases. For $|\widetilde{k}| > 0.6$ and $|\widetilde{l}| > 0.6$ it is negative (see Fig. 5b). We should also notice that in (17) the coefficient at the mixed eighth-order derivatives $\dfrac{\partial^8 u}{\partial x^4 \partial y^4}$ is equal to 0.

The transfer function for (15) has the form (see Fig. 5a):

$$f_3^5(\widetilde{k}, \widetilde{l}) = \frac{-192 \sin^2 \frac{\pi \widetilde{k}}{2} - 192 \sin^2 \frac{\pi \widetilde{l}}{2} + 512 \sin^2 \frac{\pi \widetilde{k}}{2} \sin^2 \frac{\pi \widetilde{l}}{2} + 12 \sin^2 \pi \widetilde{k} + 12 \sin^2 \pi \widetilde{l}}{36}$$
$$- \frac{16 \sin^2 \pi \widetilde{k} \sin^2 \frac{\pi \widetilde{l}}{2} + 16 \sin^2 \pi \widetilde{l} \sin^2 \frac{\pi \widetilde{k}}{2}}{36} \tag{19}$$

and its Taylor expansion containing the products of the wave-numbers $\widetilde{k}$ and $\widetilde{l}$ is presented below:

$$f_{3T}^5(\widetilde{k}, \widetilde{l}) = -\pi^2 \left(\widetilde{k}^2 + \widetilde{l}^2\right) + \frac{2\pi^4}{3} \widetilde{k}^2 \widetilde{l}^2 + \frac{\pi^6}{90}\left(\widetilde{k}^6 + \widetilde{l}^6\right) - \frac{\pi^8}{1008}\left(\widetilde{k}^8 + \widetilde{l}^8\right)$$
$$- \frac{\pi^6}{36}\left(\widetilde{k}^4 \widetilde{l}^2 + \widetilde{k}^2 \widetilde{l}^4\right) + O(\widetilde{k}^{10}, \widetilde{l}^{10}). \tag{20}$$

In the BlueNote software package added to Kupidura et al. (2010) – is presented the following rather strange mask (the Authors call it the morphological Laplacian):

$$\mathbf{Lap}_4^5 = \frac{1}{25}\begin{bmatrix} 1 & 1 & 1 & 1 & 1 \\ 1 & 1 & 1 & 1 & 1 \\ 1 & 1 & -24 & 1 & 1 \\ 1 & 1 & 1 & 1 & 1 \\ 1 & 1 & 1 & 1 & 1 \end{bmatrix}. \tag{21}$$

It is a dense matrix with no zero elements. In (21) the center pixel with the weight of $-24/25$ is surrounded by 24 pixels with the same weights equal to $1/25$.

This mask satisfies the necessary condition to be of the Laplace type: the sum of all its elements is equal to zero. The mathematical features of (21) were still unknown. Below we present the difference scheme which leads to (21):

$$\mathbb{A}_4^5 u_h = \frac{u_{i-2,j} + u_{i,j+2} + u_{i+2,j} + u_{i,j-2}}{25h^2} - \frac{24u_{i,j}}{25h^2} + \frac{u_{i-1,j} + u_{i,j+1} + u_{i+1,j} + u_{i,j-1}}{25h^2}$$
$$+ \frac{u_{i-1,j+1} + u_{i+1,j+1} + u_{i-1,j-1} + u_{i+1,j-1}}{25h^2} + \frac{u_{i-2,j+1} + u_{i+2,j+1} + u_{i-2,j-1} + u_{i+2,j-1}}{25h^2}$$
$$+ \frac{u_{i-1,j+2} + u_{i+1,j+2} + u_{i-1,j-2} + u_{i+1,j-2}}{25h^2} + \frac{u_{i-2,j-2} + u_{i-2,j+2} + u_{i+2,j-2} + u_{i+2,j+2}}{25h^2}. \tag{22}$$

We shall show that the filter mask (21) leads to the modified differential equation in which all coefficients at the mixed and unmixed even-order derivatives have the correct signs. The MDE for (22) has the form:

$$\Pi_4^5 = \nabla^2 u + \frac{17h^2}{60}\left(\frac{\partial^4 u}{\partial x^4} + \frac{\partial^4 u}{\partial y^4}\right) + h^2\frac{\partial^4 u}{\partial x^2 \partial y^2} - \frac{13h^4}{360}\left(\frac{\partial^6 u}{\partial x^6} + \frac{\partial^6 u}{\partial y^6}\right)$$

$$+ \frac{257h^6}{100800}\left(\frac{\partial^8 u}{\partial x^8} + \frac{\partial^8 u}{\partial y^8}\right) - \frac{17h^4}{60}\left(\frac{\partial^6 u}{\partial x^4 \partial y^2} + \frac{\partial^6 u}{\partial x^2 \partial y^4}\right)$$

$$+ \frac{289h^6}{3600}\frac{\partial^8 u}{\partial x^4 \partial y^4} + O(h^8). \tag{23}$$

The FDE (22) is a consistent approximation of the Laplace equation and its solution $u_h(x_i, y_j)$ converges to the exact solution $u(x, y)$. The accuracy of the difference equation (22) is of the second order. According to the spectral theory, the coefficients in front of the sums: $\frac{\partial^6 u}{\partial x^6} + \frac{\partial^6 u}{\partial y^6}$ and $\frac{\partial^8 u}{\partial x^8} + \frac{\partial^8 u}{\partial y^8}$ are correct. It is the first known twenty-five-point filter mask which satisfies this condition.

The transfer function for (20) (see Fig. 6a) and its Taylor expansion are presented below:

$$f_4^5(\widetilde{k}, \widetilde{l}) = \frac{16\left(\sin^2 \pi\widetilde{k} + \sin^2 \frac{\pi\widetilde{k}}{2}\right)\left(\sin^2 \pi\widetilde{l} + \sin^2 \frac{\pi\widetilde{l}}{2}\right)}{25}$$

$$- \frac{20\left(\sin^2 \pi\widetilde{k} + \sin^2 \pi\widetilde{l} + \sin^2 \frac{\pi\widetilde{k}}{2} + \sin^2 \frac{\pi\widetilde{l}}{2}\right)}{25}, \tag{24}$$

$$f_{4T}^5(\widetilde{k}, \widetilde{l}) = -\pi^2\left(\widetilde{k}^2 + \widetilde{l}^2\right) + \frac{17\pi^4}{60}\left(\widetilde{k}^4 + \widetilde{l}^4\right) + \pi^4\widetilde{k}^2\widetilde{l}^2 - \frac{13\pi^6}{360}\left(\widetilde{k}^6 + \widetilde{l}^6\right)$$

$$- \frac{17\pi^6}{60}\left(\widetilde{k}^4\widetilde{l}^2 + \widetilde{k}^2\widetilde{l}^4\right) + \frac{257\pi^8}{100800}\left(\widetilde{k}^8 + \widetilde{l}^8\right)$$

$$+ \frac{289\pi^8}{3600}\widetilde{k}^4\widetilde{l}^4 + O(\widetilde{k}^{10}, \widetilde{l}^{10}). \tag{25}$$

In the numerical methods and in the digital image processing there is a very well known similar but nine-point filter mask which is obtained on the basis of the finite elements method with the piecewise linear approximating functions $\mathbb{P}_1$ with a small support. Its form we present below (see Winnicki et al. (2022)):

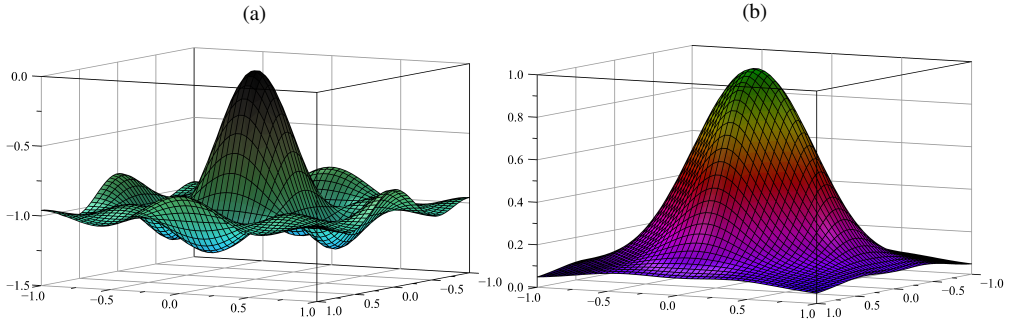$$\mathbf{K} = \frac{1}{3}\begin{bmatrix} 1 & 1 & 1 \\ 1 & -8 & 1 \\ 1 & 1 & 1 \end{bmatrix}. \tag{26}$$

(a) (b)

Fig. 6. The transfer function $f_4^5(\widetilde{k}, \widetilde{l})$ for the mask (21) – classical *Mexican hat* (negative in the entire range of $(\widetilde{k}, \widetilde{l})$) (a) and the graph of $f_4^5(\widetilde{k}, \widetilde{l})/f_L(\widetilde{k}, \widetilde{l})$ (b)

In the MDE for (26) all coefficients at the derivatives also have correct signs:

$$
\Pi_{\mathbf{K}} = \nabla^2 u + \frac{h^4}{12}\left(\frac{\partial^4 u}{\partial x^4} + \frac{\partial^4 u}{\partial y^4}\right) + \frac{h^2}{3}\frac{\partial^4 u}{\partial x^2 \partial y^2} - \frac{h^4}{360}\left(\frac{\partial^6 u}{\partial x^6} + \frac{\partial^6 u}{\partial y^6}\right)
$$
$$
- \frac{h^4}{36}\left(\frac{\partial^6 u}{\partial x^4 \partial y^2} + \frac{\partial^6 u}{\partial x^2 \partial y^4}\right) + \frac{h^6}{20160}\left(\frac{\partial^8 u}{\partial x^8} + \frac{\partial^8 u}{\partial y^8}\right) + \frac{h^6}{432}\frac{\partial^8 u}{\partial x^4 \partial y^4} + O(h^8). \quad (27)
$$

The mask (26) is also presented e.g. in Burger and Burge (2008) (page 132, with no coefficient), Lynch (2010) (page 234), Gonzalez and Woods (2018) (page 161). Prewitt (1970) and Pratt (2007) present this filter with the coefficient equal to $-1/8$.

The masks of the type (21) and (26) with one dominated center pixel react most strongly to local intensity peaks (see Section 4 – the final conclusions, conclusion 5).

Another 25-point mask is published for example in Tadeusiewicz and Korohoda (1997). It is constructed on the basis of the difference scheme:

$$
\mathbb{A}_5^5 u_h = \frac{u_{i-2,j}+u_{i,j+2}+u_{i+2,j}+u_{i,j-2}}{15h^2} - \frac{4u_{i,j}}{15h^2} - \frac{2(u_{i-1,j}+u_{i,j+1}+u_{i+1,j}+u_{i,j-1})}{15h^2}
$$
$$
+ \frac{u_{i-2,j+1}+u_{i+2,j+1}+u_{i-2,j-1}+u_{i+2,j-1}}{15h^2} + \frac{u_{i-1,j+2}+u_{i+1,j+2}+u_{i-1,j-2}+u_{i+1,j-2}}{15h^2}
$$
$$
- \frac{u_{i-1,j+1}+u_{i+1,j+1}+u_{i-1,j-1}+u_{i+1,j-1}}{30h^2} + \frac{u_{i-2,j-2}+u_{i-2,j+2}+u_{i+2,j-2}+u_{i+2,j+2}}{30h^2}. \quad (28)
$$

We present it below:

$$
\mathbf{Lap}_5^5 = \frac{1}{30}\begin{bmatrix} 1 & 2 & 2 & 2 & 1 \\ 2 & -1 & -4 & -1 & 2 \\ 2 & -4 & -8 & -4 & 2 \\ 2 & -1 & -4 & -1 & 2 \\ 1 & 2 & 2 & 2 & 1 \end{bmatrix}. \quad (29)
$$

The MDE for the difference scheme (28) is also correct and has the form:

$$
\begin{aligned}
\Pi_5^5 = \nabla^2 u &+ \frac{7h^4}{20}\left(\frac{\partial^4 u}{\partial x^4} + \frac{\partial^4 u}{\partial y^4}\right) + \frac{31h^2}{30}\frac{\partial^4 u}{\partial x^2 \partial y^2} - \frac{17h^4}{360}\left(\frac{\partial^6 u}{\partial x^6} + \frac{\partial^6 u}{\partial y^6}\right) \\
&- \frac{103h^4}{360}\left(\frac{\partial^6 u}{\partial x^4 \partial y^2} + \frac{\partial^6 u}{\partial x^2 \partial y^4}\right) + \frac{341h^6}{100800}\left(\frac{\partial^8 u}{\partial x^8} + \frac{\partial^8 u}{\partial y^8}\right) \\
&+ \frac{319h^6}{4320}\frac{\partial^8 u}{\partial x^4 \partial y^4} + O(h^8).
\end{aligned}
\tag{30}
$$

The transfer function for (28) is as follows (Fig. 7a):

$$
\begin{aligned}
f_5^5(\widetilde{k}, \widetilde{l}) &= \frac{16\sin^2 \pi\widetilde{k}\sin^2 \pi\widetilde{l} - 32(\sin^2 \pi\widetilde{k} + \sin^2 \pi\widetilde{l})}{30} \\
&+ \frac{32\left(\sin^2 \dfrac{\pi\widetilde{k}}{2}\sin^2 \pi\widetilde{l} + \sin^2 \pi\widetilde{k}\sin^2 \dfrac{\pi\widetilde{l}}{2}\right)}{30} \\
&+ \frac{8\left(\sin^2 \dfrac{\pi\widetilde{k}}{2} + \sin^2 \dfrac{\pi\widetilde{l}}{2}\right) - 16\sin^2 \dfrac{\pi\widetilde{k}}{2}\sin^2 \dfrac{\pi\widetilde{l}}{2}}{30}
\end{aligned}
\tag{31}
$$

and its Taylor expansion:

$$
\begin{aligned}
f_{5T}^5(\widetilde{k}, \widetilde{l}) = -\pi^2\left(\widetilde{k}^2 + \widetilde{l}^2\right) &+ \frac{7\pi^4}{20}\left(\widetilde{k}^4 + \widetilde{l}^4\right) + \frac{31\pi^4}{30}\widetilde{k}^2\widetilde{l}^2 \\
&- \frac{17\pi^6}{360}\left(\widetilde{k}^6 + \widetilde{l}^6\right) - \frac{103\pi^6}{360}\left(\widetilde{k}^4\widetilde{l}^2 + \widetilde{k}^2\widetilde{l}^4\right) \\
&+ \frac{341\pi^8}{100800}\left(\widetilde{k}^8 + \widetilde{l}^8\right) + \frac{319\pi^8}{4320}\widetilde{k}^4\widetilde{l}^4 + O(\widetilde{k}^{10}, \widetilde{l}^{10}).
\end{aligned}
\tag{32}
$$

For large Nyquist wave-numbers $(\widetilde{k}, \widetilde{l})$, $|\widetilde{k}| \to 1$ and $|\widetilde{l}| \to 1$ the relation $f_5^5(\widetilde{k}, \widetilde{l})/f_L(\widetilde{k}, \widetilde{l})$ is negative.

The FDE (28) is consistent and convergent as $h \to 0$ and its accuracy is of the second order. Burger and Burge (2008, p. 97) proposed another linear 5×5 pixels filter of the Laplace type:

$$
\mathbf{Lap_{BB}} = \begin{bmatrix} 0 & 0 & -1 & 0 & 0 \\ 0 & -1 & -2 & -1 & 0 \\ -1 & -2 & 16 & -2 & -1 \\ 0 & -1 & -2 & -1 & 0 \\ 0 & 0 & -1 & 0 & 0 \end{bmatrix}
\tag{$*$}
$$

and called it *Laplace* or *Mexican hat* filter. They also – rightly – used the formula: *difference filter*. But the problem is that the MDE for the difference scheme which induces this filter is incorrect:
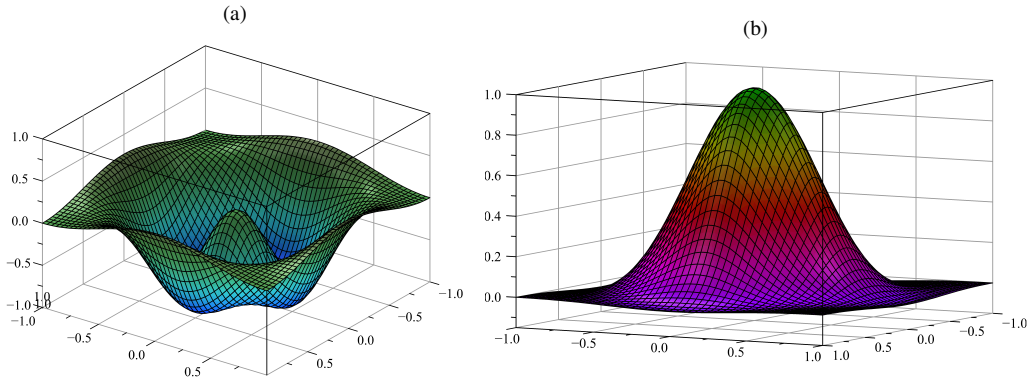
Fig. 7. The transfer function $f_5^5(\widetilde{k}, \widetilde{l})$ for the mask (29) (a) and the graph of $f_5^5(\widetilde{k}, \widetilde{l})/f_L(\widetilde{k}, \widetilde{l})$ (b)

$$\Pi_{\mathbf{BB}} = -8\nabla^2 u - \frac{5h^2}{3}\left(\frac{\partial^4 u}{\partial x^4} + \frac{\partial^4 u}{\partial y^4}\right) - h^2\frac{\partial^4 u}{\partial x^2 \partial y^2}$$
$$+ \frac{17h^4}{90}\left(\frac{\partial^6 u}{\partial x^6} + \frac{\partial^6 u}{\partial y^6}\right) + \frac{h^4}{12}\left(\frac{\partial^6 u}{\partial x^4 \partial y^2} + \frac{\partial^6 u}{\partial x^2 \partial y^4}\right)$$
$$- \frac{13h^6}{1008}\left(\frac{\partial^8 u}{\partial x^8} + \frac{\partial^8 u}{\partial y^8}\right) - \frac{h^6}{144}\frac{\partial^8 u}{\partial x^4 \partial y^4} + O(h^8). \tag{**}$$

The transfer function for (*) is graphically presented in Figure 8. The Burger and Burge *Mexican hat* filter should be modified to the following form:

$$\mathbf{Lap}_6^5 = \frac{1}{8}\begin{bmatrix} 0 & 0 & 1 & 0 & 0 \\ 0 & 1 & 2 & 1 & 0 \\ 1 & 2 & -16 & 2 & 1 \\ 0 & 1 & 2 & 1 & 0 \\ 0 & 0 & 1 & 0 & 0 \end{bmatrix}. \tag{33}$$
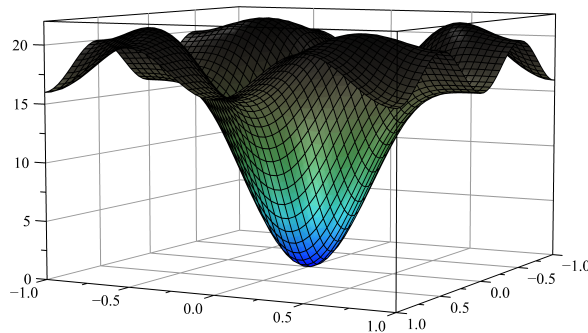

Fig. 8. The transfer function for Burger and Burge filter (*) – it is always positive
in the range of $(\widetilde{k}, \widetilde{l}) = [-1 \div 1] \times [-1 \div 1]$

The mask (33) is induced by the below presented difference scheme:

$$A_5^5 u_h = \frac{u_{i-2,j} + u_{i,j+2} + u_{i+2,j} + u_{i,j-2}}{8h^2} - \frac{2u_{i,j}}{h^2} + \frac{u_{i-1,j} + u_{i,j+1} + u_{i+1,j} + u_{i,j-1}}{4h^2}$$
$$+ \frac{u_{i-1,j+1} + u_{i+1,j+1} + u_{i-1,j-1} + u_{i+1,j-1}}{8h^2} . \tag{34}$$

In order to achieve the conformity of the mask (33) with the differential Laplace operator (1) we added the coefficient $-1/8$ to the difference scheme. Then the MDE for (34) takes the form:

$$\Pi_6^5 = \nabla^2 u + \frac{5h^2}{24} \left(\frac{\partial^4 u}{\partial x^4} + \frac{\partial^4 u}{\partial y^4} \right) + \frac{h^2}{8} \frac{\partial^4 u}{\partial x^2 \partial y^2}$$
$$- \frac{17h^4}{720} \left(\frac{\partial^6 u}{\partial x^6} + \frac{\partial^6 u}{\partial y^6} \right) - \frac{h^4}{96} \left(\frac{\partial^6 u}{\partial x^4 \partial y^2} + \frac{\partial^6 u}{\partial x^2 \partial y^4} \right)$$
$$+ \frac{13h^6}{8064} \left(\frac{\partial^8 u}{\partial x^8} + \frac{\partial^8 u}{\partial y^8} \right) + \frac{h^6}{1152} \frac{\partial^8 u}{\partial x^4 \partial y^4} + O(h^8) \tag{35}$$

and corresponds to (33) and (34).

The next step of our analysis is to present for (33) the forms of the transfer function:

$$f_6^5(\widetilde{k}, \widetilde{l}) = 2 \sin^2 \frac{\pi \widetilde{k}}{2} \sin^2 \frac{\pi \widetilde{l}}{2} - 2 \sin^2 \frac{\pi \widetilde{k}}{2} - 2 \sin^2 \frac{\pi \widetilde{l}}{2} + \frac{\sin^2 \pi \widetilde{k} + \sin^2 \pi \widetilde{l}}{2} . \tag{36}$$

(Fig. 9a) and its expansion in the Taylor series form:

$$f_{6T}^5(\widetilde{k}, \widetilde{l}) = -\pi^2 \left(\widetilde{k}^2 + \widetilde{l}^2 \right) + \frac{5\pi^4}{24} \left(\widetilde{k}^4 + \widetilde{l}^4 \right) + \frac{\pi^4}{8} \widetilde{k}^2 \widetilde{l}^2 - \frac{17\pi^6}{720} \left(\widetilde{k}^6 + \widetilde{l}^6 \right)$$
$$- \frac{\pi^6}{96} \left(\widetilde{k}^4 \widetilde{l}^2 + \widetilde{k}^2 \widetilde{l}^4 \right) + \frac{13\pi^8}{8064} \left(\widetilde{k}^8 + \widetilde{l}^8 \right) + \frac{\pi^8}{1152} \widetilde{k}^4 \widetilde{l}^4 + O(\widetilde{k}^{10}, \widetilde{l}^{10}). \tag{37}$$
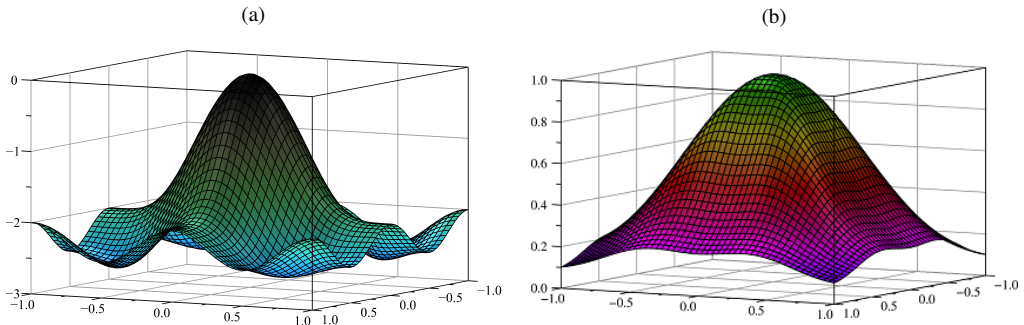

Fig. 9. The transfer function $f_6^5(\widetilde{k}, \widetilde{l})$ for the modified Burger and Burge mask (33) (negative in the entire range of $(\widetilde{k}, \widetilde{l})$) (a) and the graph of $f_6^5(\widetilde{k}, \widetilde{l})/f_L(\widetilde{k}, \widetilde{l})$ (b)

The FDE (32) is also a consistent approximation of the Laplace equation and if $h \to 0$ its solution $u_h(x_i, y_j)$ converges to the exact solution $u(x, y)$. The accuracy of the difference scheme (32) is of the second order.

The relation $f_6^5(\widetilde{k}, \widetilde{l}) / f_L(\widetilde{k}, \widetilde{l})$ for the modified Burger and Burge *Mexican hat* filter mask (31) is never negative.

2.2. *The finite element method and the fifth-order Laplace filters*

Another method of constructing the difference schemes for the partial differential equations is called the Galerkin method in which we approximate the sought after solution $u(x, y)-$ instead of the differential operator $\mathbb{A}$. The finite element method (FEM) is its particular case.

Let us consider the Poisson equation:

$$\mathbb{A}u = -\Delta u = -\sum_{k=1}^{2} \frac{\partial^2 u}{\partial x_k^2} = f(x_1, x_2), \tag{38}$$

where: $x_1 = x$ and $x_2 = y$; $u(x, y)$, $f(x, y)$ are given functions on the $\Omega = \mathbb{R} \times \mathbb{R} = [0, 1] \times [0, 1]$ domain. If $f(x, y) = 0$, the equation (38) becomes the Laplace equation.

We shall construct the difference scheme and then the filter mask of the Laplace type applying the FEM with the basis functions which are polynomials of the degree equal to 2. In this case, the functions $\varphi_i(x)$ and $\psi_j(y)$ have the forms of the Lagrange polynomials (see: Pavel et al. (2003) and Strang and Fix (2008)):

$$\varphi_i(x) = \begin{cases} 1 + 3(x - x_i)/h + 2(x - x_i)^2/h^2 & x_{i-1} \le x \le x_i \\ 1 - 3(x - x_i)/h + 2(x - x_i)^2/h^2 & x_i \le x \le x_{i+1} \\ 0 & \text{for } x \notin (x_{i-1}, x_{i+1}) \end{cases} \tag{39}$$

$$\varphi_{i-1/2}(x) = -4(x - x_i)^2/h^2 - 4(x - x_i)/h \quad x_{i-1} \le x \le x_i,$$

$$\varphi_{i+1/2}(x) = -4(x - x_i)^2/h^2 + 4(x - x_i)/h \quad x_i \le x \le x_{i+1}.$$

Equations (39) describe the piecewise parabolic approximating functions with a small support. It means that the functions vanish outside some compact subset of the Ω – Figure 10. The functions $\psi_j(y)$ have the same shape as (39) but they depend on the variable y.
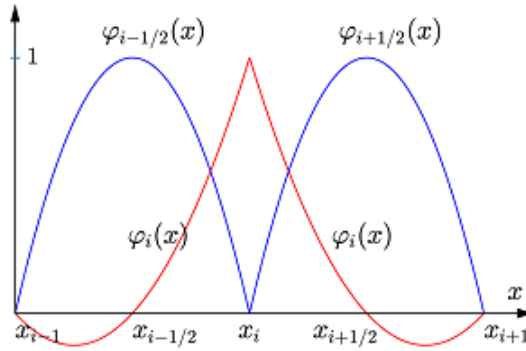
The finite element method for Lagrange $\mathbb{P}_2$ elements involves the discrete space:

$$V_h^2 = \left\{ v_h \in C^0[0, 1], \ v_h\big|_{K_{ij}} \in \mathbb{P}_2, \ 0 \le i \le N, \ 0 \le j \le N \right\}$$

and its subspace

$$V_{0,h}^2 = \left\{ v_h \in V_h^0, \ \text{such that } v_h(0) = v_h(1) = 0 \right\},$$

where: K_{ij} intervals $K_{ij} = [x_{i-1}, x_{i+1}] \times [y_{j-1, j+1}]$ forming a uniform mesh of Ω – domain in $\mathbb{R}^2$.

Fig. 10. Piecewise quadratic elements $\mathbb{P}_2$

These spaces are composed of continuous, piecewise parabolic functions. The $\mathbb{P}_2$ finite element method consists in applying the internal variational approximation approach to these spaces. The space V_h^2 is a subspace of $L^2 = L^2(\Omega)$ with the scalar product (usually integral): $(u, v)_{L^2(\Omega)} = \int_\Omega uv \, \mathrm{d}x$.

Lemma 1. *The space V_h^2 is a subspace of H^1 of dimension $2N+3$. Every function $v_h \in V_h^2$ is uniquely defined by its values at the mesh vertices $(x_i)_{0 \le i \le N+1}$ and at the midpoints $(x_{i+1/2})_{0 \le i \le N}$:*

$$v_h(x) = \sum_{i=0}^{N+1} v_h(x_i)\varphi_i(x) + \sum_{i=0}^{N} v_h(x_{i+1/2})\varphi_{i+1/2}(x) : \quad \forall x \in [x_{i-1}, x_{i+1}],$$

where (φ_i) is the basis of the shape functions defined as (39).

Remark 1. Notice that we have:

$$\begin{aligned}
\varphi_i(x_i) &= \delta_{ij}, & \varphi_i(x_{i\pm1}) &= 0, \\
\varphi_i(x_{i\pm1/2}) &= 0, & \varphi_{i-1/2}(x_{i-1/2}) &= \delta_{ij}, \\
\varphi_{i\pm1/2}(x_i) &= 0, & \varphi_{i+1/2}(x_{i+1/2}) &= \delta_{ij}, \\
\varphi_{i-1/2}(x_{i-1}) &= 0, & \varphi_{i+1/2}(x_{i+1}) &= 0.
\end{aligned}$$

The above functions are also called the Lagrange $\mathbb{P}_2$ elements. In 2-dimensional cases the variational formulation of (43) is to find such $u(x, y) \in H_0^1$ (H_0^1 Sobolev space) that for $\forall \xi(x, y) \in H_0^1$:

$$\int_\Omega \mathbb{A}u\xi \, \mathrm{d}\Omega = -\int_\Omega \Delta u\xi \, \mathrm{d}\Omega = \int_\Omega f\xi \, \mathrm{d}\theta, \tag{40}$$

where: $\xi(x, y)$ – so called test function. Applying the Green formula for integrating by parts to (40) we obtain:

$$\int_\Omega \sum_{i=1}^{2} D_i u D_i \xi \, \mathrm{d}\Omega - \int_{\partial\Omega} \frac{\partial u}{\partial n} \xi \, \mathrm{d}\Gamma = \int_\Omega f\xi \, \mathrm{d}\Omega, \tag{41}$$

where: $D_1 = \dfrac{\partial}{\partial x}$, $D_2 = \dfrac{\partial}{\partial y}$ and $\dfrac{\partial u}{\partial n} = \nabla u \cdot \mathbf{n} = \sum_{i=1}^{2} \dfrac{\partial u}{\partial x_i} n_i$ denotes the normal derivative of u on $\partial \Omega$. The expression:

$$a(u, \xi) = \int_{\Omega} \sum_{i=1}^{2} D_i u D_i \xi \, d\Omega \tag{42}$$

leads to the discrete approximation for the Laplace operator:

$$
\begin{aligned}
\mathbb{A}_7^5 u_h = {}& \frac{u_{i-1,j+1} - 16u_{i-1/2,j+1} + 30u_{i,j+1} - 16u_{i+1/2,j+1} + u_{i+1,j+1}}{144h^2} \\
&- \frac{16u_{i-1,j+1/2} - 256u_{i-1/2,j+1/2} + 480u_{i,j+1/2} - 256u_{i+1/2,j+1/2} + 16u_{i+1,j+1/2}}{144h^2} \\
&+ \frac{30u_{i-1,j} - 480u_{i-1/2,j} + 900u_{i,j} - 480u_{i+1/2,j} + 30u_{i+1,j}}{144h^2} \\
&- \frac{16u_{i-1,j-1/2} - 256u_{i-1/2,j-1/2} + 480u_{i,j-1/2} - 256u_{i+1/2,j-1/2} + 16u_{i+1,j-1/2}}{144h^2} \\
&+ \frac{u_{i-1,j-1} - 16u_{i-1/2,j-1} + 30u_{i,j-1} - 16u_{i+1/2,j-1} + u_{i+1,j-1}}{144h^2}
\end{aligned}
\tag{43}
$$

and to the filter mask:

$$\mathbf{Lap}_7^5 = \frac{1}{144}
\begin{bmatrix}
1 & -16 & 30 & -16 & 1 \\
-16 & 256 & -480 & 256 & -16 \\
30 & -480 & 900 & -480 & 30 \\
-16 & 256 & -480 & 256 & -16 \\
1 & -16 & 30 & -16 & 1
\end{bmatrix}. \tag{44}$$

Detailed analysis leads us to the conclusion that neither the difference scheme (43) approaches the Laplace operator nor the filter mask (44) is directly connected with the filter of the Laplace type. The MDE for the difference scheme (43) is induced by the mixed fourth-order derivatives – one of the terms of the biharmonic equation:

$$\Pi_7^5 = h^4 \frac{\partial^4 u}{\partial x^2 \partial y^2} + O(h^6) \tag{45}$$

and not by the standard Laplace differential operator: $\mathbb{A}u = \dfrac{\partial^2 u}{\partial x^2} + \dfrac{\partial^2 u}{\partial y^2}$.

It is a similar case to that discussed in Thompson (1955a). We presented there a filter mask in the form:

$$\mathbf{FM} =
\begin{bmatrix}
1 & -2 & 1 \\
-2 & 4 & -2 \\
1 & -2 & 1
\end{bmatrix} \tag{46}$$

for which the MDE was also equal to (45):

$$\Pi_{\mathbf{FM}} = h^4 \frac{\partial^4 u}{\partial x^2 \partial y^2} + O(h^6). \tag{47}$$

The filter mask (44) was also presented by Tadeusiewicz and Korohoda (1997), Pratt (2007) (page 503), Prewitt (1970) (page 126) and Borawski (2004). Applying the Lagrange $\mathbb{P}_2$ elements does not mean that we cannot construct the difference scheme for the Laplace equation in 2-D.

Let us return to the difference scheme (6). The vector $\begin{bmatrix} -1 & 16 & -30 & 16 & -1 \end{bmatrix}$ approaches the second-order derivative $\dfrac{\partial^2 u}{\partial x^2}$ in V_h^2. The elementary contributions of each element K_{ij} to the stiffness matrix can be derived (Strang and Fix, 2008):

$$
\begin{bmatrix}
7 & -8 & 1 & 0 & 0 \\
-8 & 16 & -8 & 0 & 0 \\
1 & -8 & 7 & 0 & 0 \\
0 & 0 & 0 & 0 & 0 \\
0 & 0 & 0 & 0 & 0
\end{bmatrix}
+
\begin{bmatrix}
0 & 0 & 0 & 0 & 0 \\
0 & 7 & -8 & 1 & 0 \\
0 & -8 & 16 & -8 & 0 \\
0 & 0 & 0 & 0 & 0 \\
0 & 0 & 0 & 0 & 0
\end{bmatrix}
+
\begin{bmatrix}
0 & 0 & 0 & 0 & 0 \\
0 & 0 & 0 & 0 & 0 \\
0 & 0 & 7 & -8 & 1 \\
0 & 0 & -8 & 16 & -8 \\
0 & 0 & 1 & -8 & 7
\end{bmatrix}
$$

$$
=
\begin{bmatrix}
7 & -8 & \boxed{1} & 0 & 0 \\
-8 & 23 & \boxed{-16} & 0 & 0 \\
\boxed{1} & \boxed{-8} & \boxed{30} & \boxed{-16} & \boxed{1} \\
0 & 1 & \boxed{-16} & 23 & -8 \\
0 & 0 & \boxed{1} & -8 & 7
\end{bmatrix}. \tag{48}
$$

In effect we can obtain the difference scheme which is equivalent to the FDE (5) and the filter mask (6) proposed by the scientists mentioned in the beginning of this section.

3. The numerical tests

Let us carry out a numerical test. Figure 11a presents a field of any function $I(x, y)$ determined by the script *peaks.m* in which one can appoint strong gradient, weak gradient and gradient-less areas of the function $I(x, y)$. Let us filter this field by the 5×5 pixels Laplace mask $\mathbf{Lap}_1^5$ (6) derived on the basis of the fourth-order difference scheme (5) (Fig. 11b) and then by the 3×3 pixels mask $\mathbf{Lap}_3^3$:

$$\mathbf{Lap}_3^3 = \frac{1}{6}\begin{bmatrix} 1 & 4 & 1 \\ 4 & -20 & 4 \\ 1 & 4 & 1 \end{bmatrix}, \qquad \mathbf{Lap}_1^3 = \begin{bmatrix} 0 & 1 & 0 \\ 1 & -4 & 1 \\ 0 & 1 & 0 \end{bmatrix} \tag{49}$$

also derived on the basis of the fourth-order difference scheme (Fig. 11c) (Miyakoda, 1960; Strikwerda, 2004 (pages 328, 331); LeVeque, 2007; Winnicki et al., 2022).
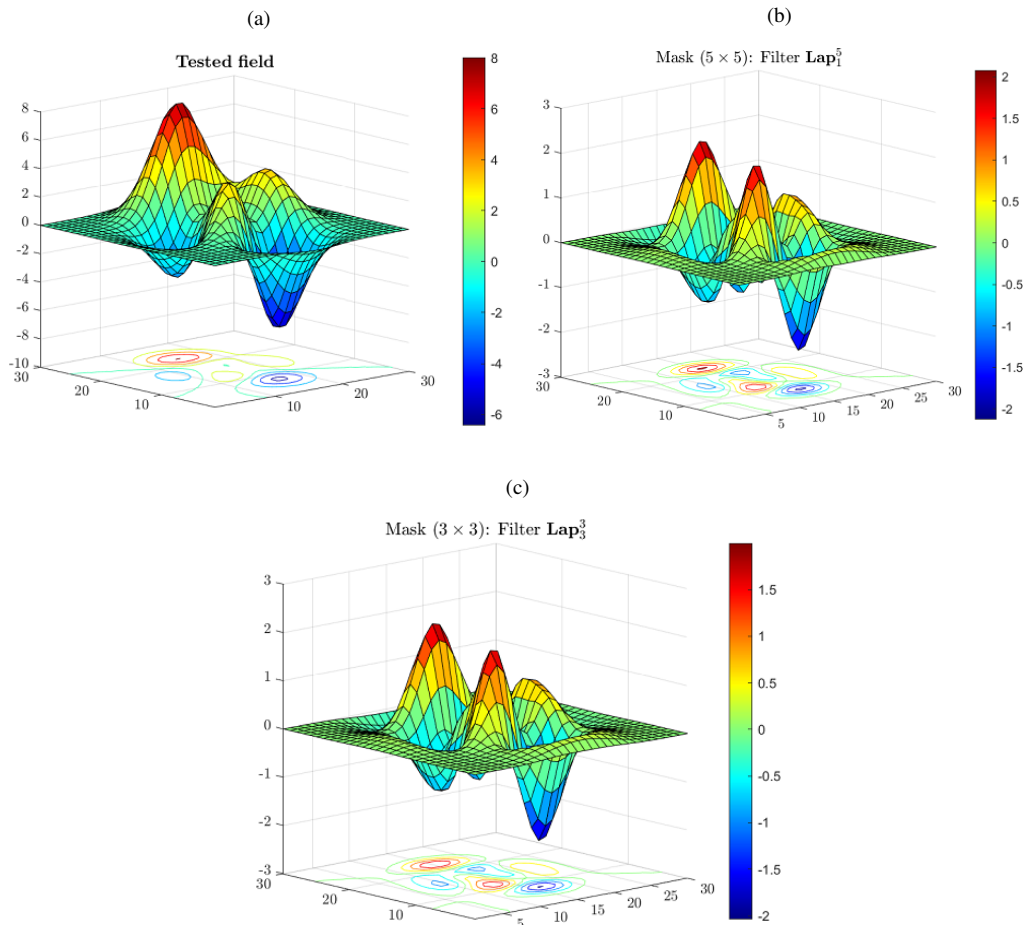
Fig. 11. Tested field (a), the tested field after filtering by means of the mask (6) (b) and the tested field after filtering by means of the mask (47) (c)

The natural feature of the filter masks of the Laplace type is that they generally highlight regions of rapid changes of the function $I(x, y)$ values.

The gradients of these changes are clearly seen as the isolines of the vertical projections of the tested and filtered fields of *peaks.m* on the horizontal plane in Figure 11. The Laplace filters sharpen the gradients but, unfortunately, they usually reduce the maxima and the minima of the magnitudes of any fluctuation (compare the ranges of the color bars in Figure 11a, 11b, 11c). In general, the shape of the tested field is conserved.

Let us also note that the filter masks (44) and (46) cut all the fluctuations in the analyzed fields (Fig 12a and Fig. 12b, respectively). The magnitudes of the remaining fluctuations are less than |0.11| for filter (44) and about |0.12| for filter (46), respectively, while the maximum of the magnitude of the test field in Fig. 11a is approximately equal to |8.02|. So, in our opinion the presented example is the best proof that the masks (44)

and (46) are not of the Laplace type. The sums of all elements of these filters are equal to zero, however, it is the feature of all kernels applied to corners and edges of objects detection.
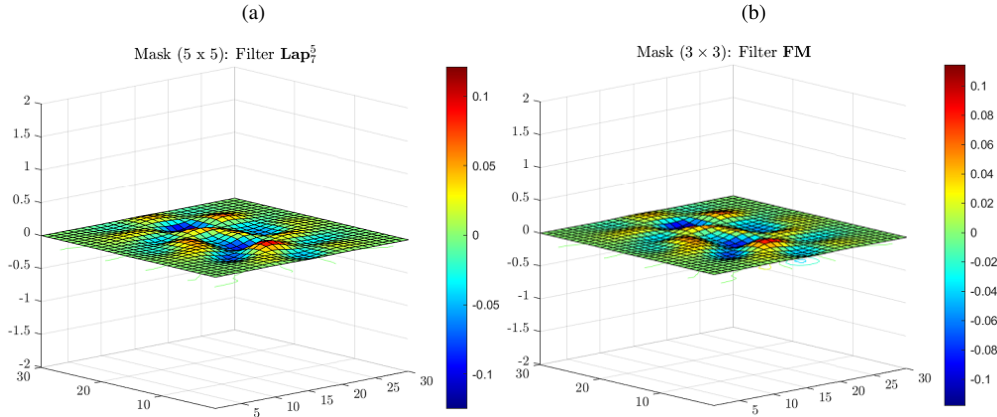

Fig. 12. The tested field after filtering by means of the mask: (44) (a) and the tested field after filtering by means of the mask: (46) (b)

The graphs of the cross sections of the transfer functions: $f_P(\widetilde{k}, \widetilde{l})/f_L(\widetilde{k}, \widetilde{l})$ for some $\widetilde{l} = \text{const} \in (0 \div 1)$ are presented in Figure 13.
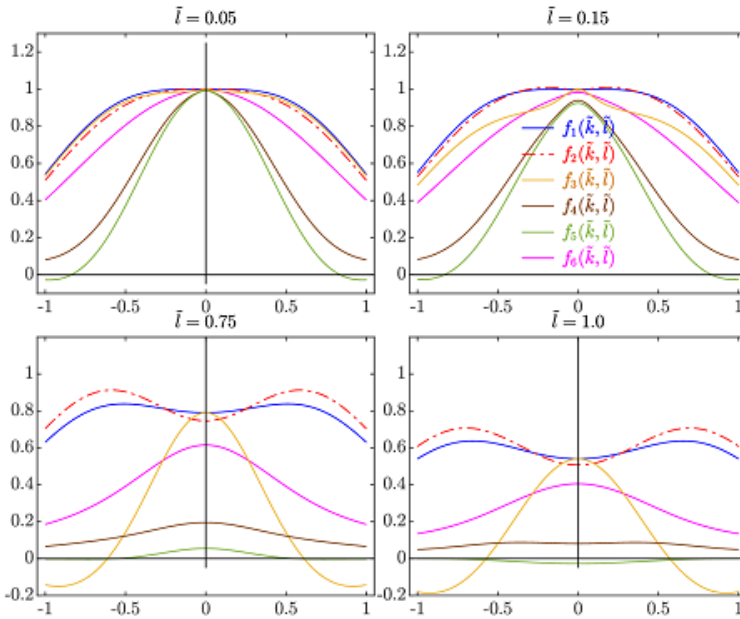
Fig. 13. The graphs of the functions $\dfrac{f_P(\widetilde{k}, \widetilde{l} = \text{const})}{f_L(\widetilde{k}, \widetilde{l} = \text{const})}$ for $\widetilde{l} = 0.05, \widetilde{l} = 0.15, \widetilde{l} = 0.75, \widetilde{l} = 1.0,\ p = 1 \pm 6$

In Figure 14 we present the graphs of $f_1^5(\widetilde{k}, \widetilde{l})$ – blue line, the transfer function $f_3(\widetilde{k}, \widetilde{l}) = \frac{8}{3}\sin^2\frac{\pi\widetilde{k}}{2}\sin^2\frac{\pi\widetilde{l}}{2} - 4\sin^2\frac{\pi\widetilde{k}}{2} - 4\sin^2\frac{\pi\widetilde{l}}{2}$ for the filter **Lap**$_3^3$ (49) – magenta line and the transfer function $f_1^3(\widetilde{k}, \widetilde{l}) = -4\sin^2\frac{\pi\widetilde{k}}{2} - 4\sin^2\frac{\pi\widetilde{l}}{2}$ for **Lap**$_1^3$ (49) based on the "cross" stencil (the first difference proposition for the Laplacian, see Richardson (1910)) – green line. We shall discuss these graphs in both figures in Section 4.
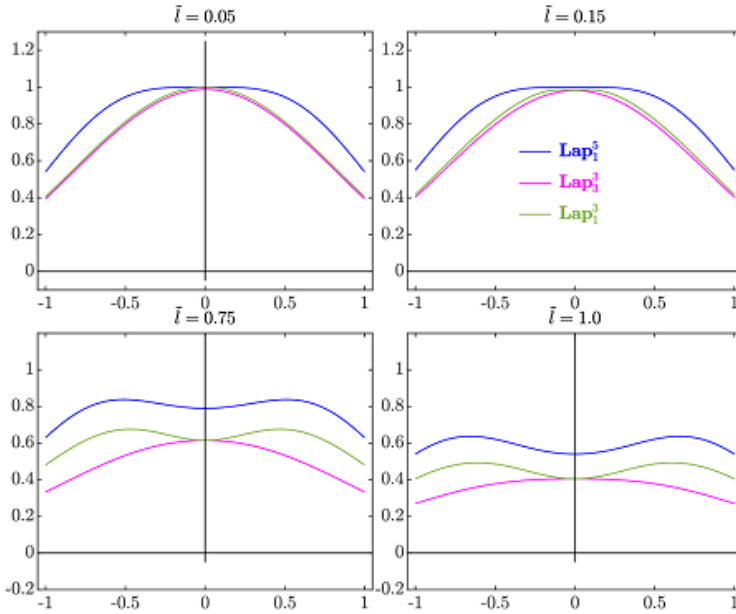
Fig. 14. As above but only for the masks (6) and both (49)

A few plane figures: square, triangle, pentagon, parallelogram, star, square with rounded corners (squircle), cross and rhombus are presented in Figure 15a. The same
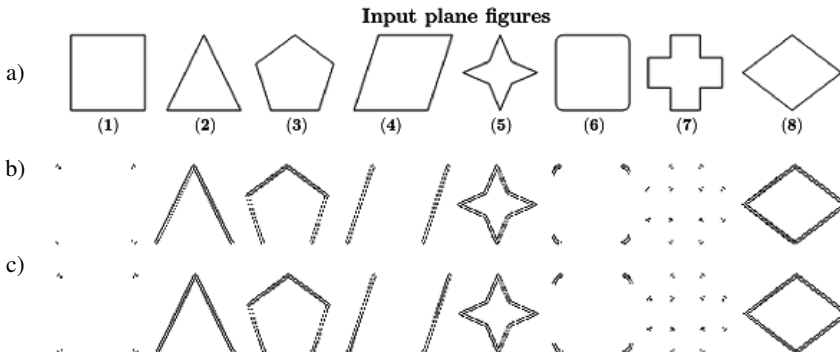
Fig. 15. The differences in filtering the plane geometrical figures (a) by means of the masks (44) (b) and (46) are unnoticeable (c)

plane figures after filtering by means of the masks (44) and (46) are presented in Figure 15b and Figure 15c, respectively.

Table 1. Masks of the fifth-order filters and their first differential approximations (f.d.a).
The coefficients of the terms in red have incorrect signs

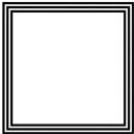| Masks	The shortened Π-forms of the the f.d.a – MDE:
$\dfrac{1}{12}\begin{bmatrix} 0 & 0 & -1 & 0 & 0 \\ 0 & 0 & 16 & 0 & 0 \\ -1 & 16 & -60 & 16 & -1 \\ 0 & 0 & 16 & 0 & 0 \\ 0 & 0 & -1 & 0 & 0 \end{bmatrix}$	$\Pi_1^5 = \nabla^2 u - \dfrac{h^4}{90}\left(\dfrac{\partial^6 u}{\partial x^6} + \dfrac{\partial^6 u}{\partial y^6}\right) - \dfrac{h^6}{1008}\left(\dfrac{\partial^8 u}{\partial x^8} + \dfrac{\partial^8 u}{\partial y^8}\right) + O(h^8)$
$\dfrac{1}{16}\begin{bmatrix} 0 & 0 & -1 & 0 & 0 \\ 0 & -2 & 24 & -2 & 0 \\ -1 & 24 & -84 & 24 & -1 \\ 0 & -2 & 24 & -2 & 0 \\ 0 & 0 & -1 & 0 & 0 \end{bmatrix}$	$\Pi_2^5 = \nabla^2 u + \dfrac{h^2}{48}\left(\dfrac{\partial^4 u}{\partial x^4} + \dfrac{\partial^4 u}{\partial y^4}\right) - \dfrac{h^2}{8}\dfrac{\partial^4 u}{\partial x^2 \partial y^2}$ $+ \dfrac{11h^4}{1440}\left(\dfrac{\partial^6 u}{\partial x^6} + \dfrac{\partial^6 u}{\partial y^6}\right) - \dfrac{h^4}{96}\left(\dfrac{\partial^6 u}{\partial x^4 \partial y^2} + \dfrac{\partial^6 u}{\partial x^2 \partial y^4}\right)$ $- \dfrac{h^6}{1152}\dfrac{\partial^8 u}{\partial x^4 \partial y^4} - \dfrac{59h^6}{80640}\left(\dfrac{\partial^8 u}{\partial x^8} + \dfrac{\partial^8 u}{\partial y^8}\right) + O(h^8)$
$\dfrac{1}{36}\begin{bmatrix} 0 & -1 & -1 & -1 & 0 \\ -1 & 32 & -14 & 32 & -1 \\ -1 & -14 & -60 & -14 & -1 \\ -1 & 32 & -14 & 32 & -1 \\ 0 & -1 & -1 & -1 & 0 \end{bmatrix}$	$\Pi_3^5 = \nabla^2 u + \dfrac{2h^2}{3}\dfrac{\partial^4 u}{\partial x^2 \partial y^2} + \dfrac{h^4}{90}\left(\dfrac{\partial^6 u}{\partial x^6} + \dfrac{\partial^6 u}{\partial y^6}\right) - \dfrac{h^6}{1008}\left(\dfrac{\partial^8 u}{\partial x^8} + \dfrac{\partial^8 u}{\partial y^8}\right)$ $- \dfrac{h^4}{36}\left(\dfrac{\partial^6 u}{\partial x^4 \partial y^2} + \dfrac{\partial^6 u}{\partial x^2 \partial y^4}\right) + O(h^8)$
$\dfrac{1}{25}\begin{bmatrix} 1 & 1 & 1 & 1 & 1 \\ 1 & 1 & 1 & 1 & 1 \\ 1 & 1 & -24 & 1 & 1 \\ 1 & 1 & 1 & 1 & 1 \\ 1 & 1 & 1 & 1 & 1 \end{bmatrix}$	$\Pi_4^5 = \nabla^2 u + \dfrac{17h^2}{60}\left(\dfrac{\partial^4 u}{\partial x^4} + \dfrac{\partial^4 u}{\partial y^4}\right) + h^2\dfrac{\partial^4 u}{\partial x^2 \partial y^2} - \dfrac{13h^4}{360}\left(\dfrac{\partial^6 u}{\partial x^6} + \dfrac{\partial^6 u}{\partial y^6}\right)$ $+ \dfrac{257h^6}{100800}\left(\dfrac{\partial^8 u}{\partial x^8} + \dfrac{\partial^8 u}{\partial y^8}\right)$ $- \dfrac{17h^4}{60}\left(\dfrac{\partial^6 u}{\partial x^4 \partial y^2} + \dfrac{\partial^6 u}{\partial x^2 \partial y^4}\right) + \dfrac{289h^6}{3600}\dfrac{\partial^8 u}{\partial x^4 \partial y^4} + O(h^8)$
$\dfrac{1}{30}\begin{bmatrix} 1 & 2 & 2 & 2 & 1 \\ 2 & -1 & -4 & -1 & 2 \\ 2 & -4 & -8 & -4 & 2 \\ 2 & -1 & -4 & -1 & 2 \\ 1 & 2 & 2 & 2 & 1 \end{bmatrix}$	$\Pi_5^5 = \nabla^2 u + \dfrac{7h^4}{20}\left(\dfrac{\partial^4 u}{\partial x^4} + \dfrac{\partial^4 u}{\partial y^4}\right) + \dfrac{31h^2}{30}\dfrac{\partial^4 u}{\partial x^2 \partial y^2} - \dfrac{17h^4}{360}\left(\dfrac{\partial^6 u}{\partial x^6} + \dfrac{\partial^6 u}{\partial y^6}\right)$ $- \dfrac{103h^4}{360}\left(\dfrac{\partial^6 u}{\partial x^4 \partial y^2} + \dfrac{\partial^6 u}{\partial x^2 \partial y^4}\right) + \dfrac{341h^6}{100800}\left(\dfrac{\partial^8 u}{\partial x^8} + \dfrac{\partial^8 u}{\partial y^8}\right)$ $+ \dfrac{319h^6}{4320}\dfrac{\partial^8 u}{\partial x^4 \partial y^4} + O(h^8)$
$\dfrac{1}{8}\begin{bmatrix} 0 & 0 & 1 & 0 & 0 \\ 0 & 1 & 2 & 1 & 0 \\ 1 & 2 & -16 & 2 & 1 \\ 0 & 1 & 2 & 1 & 0 \\ 0 & 0 & 1 & 0 & 0 \end{bmatrix}$	$\Pi_6^5 = \nabla^2 u + \dfrac{5h^2}{24}\left(\dfrac{\partial^4 u}{\partial x^4} + \dfrac{\partial^4 u}{\partial y^4}\right) + \dfrac{h^2}{8}\dfrac{\partial^4 u}{\partial x^2 \partial y^2} - \dfrac{17h^4}{720}\left(\dfrac{\partial^6 u}{\partial x^6} + \dfrac{\partial^6 u}{\partial y^6}\right)$ $- \dfrac{h^4}{96}\left(\dfrac{\partial^6 u}{\partial x^4 \partial y^2} + \dfrac{\partial^6 u}{\partial x^2 \partial y^4}\right)$ $+ \dfrac{13h^6}{8064}\left(\dfrac{\partial^8 u}{\partial x^8} + \dfrac{\partial^8 u}{\partial y^8}\right) + \dfrac{h^6}{1152}\dfrac{\partial^8 u}{\partial x^4 \partial y^4} + O(h^8)$

Note that in Figure 15b and Figure 15c all horizontal and vertical edges were removed from the figures by the masks (44) and (46): all edges in the square (Fig. 15b1 and Fig. 15c1), the bases of the triangle (Fig. 15b2 and Fig. 15c2), pentagon (Fig. 15b3 and Fig. 15c3) and parallelogram (Fig. 15b4 and Fig. 15c4, here also the upper edge). The analyzed masks also removed wide fragments of the horizontal and vertical edges of the squircle (Fig. 15b6 and Fig. 15c6). The star (Fig. 15b5 and Fig. 15c5) and the rhombus (Fig. 15b8 and Fig. 15c8) are not changed because their edges are neither horizontal nor vertical.

The most interesting plane figure is the cross (Fig. 15a7) where filtering its image reduced all horizontal and vertical linear structures to the corner pixels (Fig. 15b7 and Fig. 15c7).

In our analysis we come to the conclusion that the filter masks (44) and (46) are not isotropic. They strongly depend on the edges orientation. If the edges are neither horizontal nor vertical the filter masks (44) and (46) are "blind" to all contours (see for example the triangle, pentagon, parallelogram, star and rhombus). Therefore, the masks (44) and (46) must not be called filter masks of the Laplace type (the Laplace kernels highlight the edges).

The results of another test presented in Table 2 confirm that the differences in filtering of the plane geometrical figures (single and triple squares) by means of the masks (44) and (46) are hardly noticeable. Because the calculations with the 5×5 pixel mask are more expensive than with the 3×3 pixel mask, we suggest that the mask (46) should be applied to filtering large digital images.

Table 2. Detection of the corners of the single and triple squares

Lap$_7^5$ (44)		
FM (46)		

The masks (44) and (46) could be an alternative to the Harris corner detector method for digital image processing applied to figures with horizontal and vertical edges (see: Marr and Hildreth (1980), Harris and Stephens (1988), Burger and Burge (2008).

4. The final conclusions

We discussed the spectral features of seven filter masks of the fifth order for the Laplace differential operator $\mathrm{A}u = \dfrac{\partial^2 u}{\partial x^2} + \dfrac{\partial^2 u}{\partial y^2}$. Six of them were derived on the basis of the finite difference method and one on the basis of the finite element method with approximation of the solution $u(x, y)$ by means of the piecewise quadratic Lagrange $\mathbb{P}_2$ elements (see (44)). The MDEs (Table 1) and the transfer functions for each of them were also presented here. It turns out that the filter mask (44), alike the filter (46) is not induced by the Laplace operator but by the mixed derivatives of the fourth order: $\dfrac{\partial^4 u}{\partial x^2 \partial y^2}$.

In numerical methods the difference schemes spread on five points in each direction are not too popular, even these of the fourth-order accuracy (6). They render too many points near boundaries, even in regular grid. The main problem concerns the boundary conditions.

Our analysis yields a few conclusions:

1. All the presented Laplace masks satisfy the standard condition (and the necessary condition) for the Laplace difference operator and for the Laplace filters: the sum of all elements of the filters $\mathbf{Lap}_1^5 \div \mathbf{Lap}_6^5$ is equal to zero.

2. The Laplace filter $\mathbf{Lap}_1^5$ (6) is characterized by the best conformity of its transfer function $f_1^5(\widetilde{k}, \widetilde{l})$ (8) to the transfer function of the Laplace differential operator $f_L(\widetilde{k}, \widetilde{l})$ for the full range of $(\widetilde{k}, \widetilde{l}) = [-1 \div 1] \times [-1 \div 1]$ and in general it is much better than for the 3×3 pixels masks – Figure 12. Let us also notice that the filters $\mathbf{Lap}_1^5$ (6) and $\mathbf{Lap}_1^3$ (49) have the simplest structure: they are based on the "cross" 25-point and 9-point stencils, respectively, and they have no mixed derivatives in their MDEs. Every mask of the Laplace type with coefficients only on the "cross" stencil yields lower costs of calculations.

3. The transfer function $f_2^5(\widetilde{k}, \widetilde{l})$ (13) – Figure 11, red dot-dashed line – for medium Nyquist wave-numbers exceeds 1, see also Figure 3. The choice between the masks (6) and (11) depends on the structure of the digital images.

4. The application of the Laplace type mask $\mathbf{Lap}_3^5$ (16) is rather limited. For medium and large Nyquist wave-numbers its transfer function $f_3^5(\widetilde{k}, \widetilde{l})$ (19) is negative (Fig. 11 – orange line). We come to the same conclusion with respect to the mask $\mathbf{Lap}_5^5$ (29) (Fig. 11 – green line).

5. Our analysis has shown that the filter (26) most strongly cuts the local intensity peaks in the family of the third-order masks (from $[-6.43 \div 8.02]$ to $[-2.02 \div 1.98]$) and the filter (22) in the family of the fifth-order masks (from $[-6.43 \div 8.02]$ to $[-1.79 \div 1.77]$).

The first differential approximations for the analyzed filter masks of the Laplace type are collected in Table 1 where we additionally marked the coefficients with incorrect signs in red.

Author contributions

Conceptualization: I.W.; methodology: S.P. and K.K.; validation: J.J. and K.K.; writing original draft preparation: I.W.; writing-review and editing: J.J; supervision: I.W.; project administration: I.W.; funding acquisition: J.J.

Data availability statement

No datasets were used in this research.

References

Appadu, A.R., Dauhoo, M.Z., Rughooputh, S.D.D.V. (2008). Control of numerical effects of dispersion and dissipation in numerical schemes for efficient shock-capturing through an optimal Courant number. *Comput. Fluids*, 37(6), 767–783. DOI: 10.1016/j.compfluid.2007.07.018.

Appadu, A.R., and Dauhoo, M.Z. (2011). The Concept of Minimized Integrated Exponential Error for Low Dispersion and Low Dissipation Schemes. *Int. J. Numerical Methods Fluids*, 65(5), 578–601. DOI: 10.1002/fld.2206.

Appadu, A.R. (2014). Optimized Low Dispersion and Low Dissipation Runge–Kutta Algorithms in Computational Aeroacoustics. *Appl. Math. Inf. Sci.*, 8(1), 57–68. DOI: 10.12785/amis/080106.

Borawski, M. (2004). *Preliminary digital image processing*. In: Methods of Comparative Navigation (in Polish), 88–119. Gdynia: Andrzej Stateczny GTN.

Burger, W., and Burge, M.J. (2008). *Digital Image Processing. An Algorithmic Introduction Using Java. Texts in Computer Science*. New York: Springer Science + Business Media.

Burger, W., and Burge, M.J. (2009a). Principles of Digital Image Processing. Core Algorithms. London: Springer–Verlag.

Burger, W., and Burge, M.J. (2009b). Principles of Digital Image Processing. Fundamental Techniques. London: Springer–Verlag.

Fryskowska, A., Kedzierski, M., Wierzbicki, D. et al. (2019). Analysis of imagery interpretability of open sources radar satellite imagery. In: Proceedings of 12th Conference on Reconnaissance and Electronic Warfare Systems (CREWS). Oltarzew (2019). DOI: 10.1117/12.2525013.

Gates, W.L. (1956). On the truncation error, stability, and convergence of difference solutions of the barotropic vorticity equation. *J. Meteorol.*, 16, 556–568.

Gates, W.L. (1961). The reduction of truncation error by extrapolation techniques. *Mon. Wea. Rev.*, 89, 115–124. DOI: 10.1175/1520-0493(1961)089<0115:TROTEB>2.0.CO;2

Gonzalez, R.C., and Woods, R.E. (2018). *Digital Image Processing, 4 edn. Pearson International Edition*. New Jersey: Pearson Education.

Harris, C., and Stephens, M. (1988). *A combined corner and edge detector*. In Taylor C.J. (Eds.) Proceedings of the Alvey Vision Conference, p. 23. 1–23.6. DOI: 10.5244/C.2.23.

Iserles, A. (2009). *A First Course in the Numerical Analysis of Differential Equations*. Cambridge: University Press.

Jähne, B., Scharr, H., Körkel, S. et al. (1999). *Principles of filter design*. In: Handbook of computer vision and applications, 2, 125–151. Academic Press.

Jähne, B. (2002). Digital Image Processing. Berlin: Springer–Verlag.

Jasinski, J., Kroszczynski, K., Rymarz, C. et al. (1999). Satellite Images of Atmospheric Processes Moulding Weather (in Polish). Warsaw: PWN.

Knighting, E. (1955). *Reduction of truncation errors in symmetrical operators*. Technical Memorandum of the Joint Numerical Weather Prediction Unit, 3(5).

Krawczyk, K., Winnicki, I., Pietrek, S. et al. (2012). Spectral properties of fifth order Laplace filters used for digital data processing. *Bulletin of the Military University of Technology*, 61(1), 145–170.

Kupidura, A, and Kupidura, P. (2009). Investigating urban sprawl using remote sensing and GIS technology. In: Proceedings of 29th EARSeL Symposium, 224–230. Chania, Greece (2009).

Kupidura, P., Koza, P., Marciniak, J. (2010). Mathematical Morphology in Remote Sensing (in Polish). Warsaw: PWN.

Kurczynski, Z., Rozycki, S., Bylina, P. (2017). Mapping of polar areas based on high-resolution satellite images: the example of the Henryk Arctowski Polish Antarctic Station. *Reports Geod. Geoinf.*, 104(1), 65–78. DOI: 10.1515/rgg-2017-0016.

LeVeque, R.J. (2007). *Finite Difference Methods for Ordinary and Partial Differential Equations. Steady-State and Time-Dependent Problems*. Philadelphia: SIAM. DOI: 10.1137/1.9780898717839.

Li, J., and Yang, Z. (2011). Heuristic modified equation analysis on oscillations in numerical solutions of conservation laws. *SIAM J. Numer. Anal.*, 49, 2386–2406. DOI: 10.1137/110822591.

Li, J., and Yang, Z. (2013). The von Neumann analysis and modified equation approach for finite difference schemes. *Appl. Math. Comput.*, 225, 610–621. DOI: 10.1016/j.amc.2013.09.046.

Lynch, D.R. (2010). *Numerical Partial Differential Equations for Environmental Scientists and Engineers: A First Practical Course*. New York: Springer Science + Business Media. DOI: 10.1121/1.1577548.

Mallat, S. (2009). *A Wavelet Tour of Signal Processing. The Sparse Way*. Amsterdam: Academic Press.

Marr, D., and Hildreth, E. (1980). Theory of edge detection. *Proc. Royal Soc.*, 207, 187–217. DOI: 10.1098/rspb.1980.0020.

Miyakoda, K. (1960). Numerical calculation of Laplacian and Jacobian using 9 and 25 gridpoint systems. *J. Meteorol. Soc. Japan*, 2, 94–105.

Ogura, Y. (1958). On the truncation error which arises from the use of finite differences in the Laplacian operator. *J. Meteorol.*, 15(5), 475–480. DOI: 10.1175/1520-0469(1958)015<0475:OTTEWA>2.0.CO;2.

Parker, J.R. (2011). *Algorithms for Image Processing and Computer Vision*. Indianapolis: Wiley.

Pavel, S., Segeth, K., Dolezel, I. (2003). *Higher-Order Finite Element Methods*. Chapman & Hall/CRC.

Petrou, M., and Petrou, C. (2011). *Image Processing. The Fundamentals*. Chichester: John Wiley & Sons.

Peyret, R., and Taylor, T.D. (1983). *Computational Methods for Fluid Flow*. New York: Springer-Verlag.

Pitas, I. (2000). *Digital Image Processing Algorithms and Applications*. New York: John Wiley & Sons.

Pokonieczny, K., and Moscicka, A. (2018). The influence of the shape and size of the cell on developing military passability maps. *ISPRS Int. J. Geoinf.*, 7(7). DOI: 10.3390/ijgi7070261.

Pratt, W.K. (2007). Digital Image Processing. New York: Wiley-Interscience.

Prewitt, J.M.S. (1970). *Object enhancement and extraction*. In: B.S. Lipkin and A. Rosenfeld. (Eds.) Picture Processing and Psychopictorics, 75–150. New York: Academic Press.

Reda, K., and Kedzierski, M. (2020). Detection, classification, and boundary regularization of buildings in satellite imagery using faster edge region convolutional neural networks. *Remote Sens.*, 12(14). DOI: 10.3390/rs12142240.

Richardson, L.F. (1910). The approximate arithmetical solution by finite differences of physical problems involving differential equations, with an application to the stresses in a masonry dam. *Philos. Proc. R. Soc. London Ser.* A, 210, 307–357.

Scharr, H. (2000). *Optimal operators in digital image processing. Ph.D. thesis*. Interdisciplinary Center for Scientific Computing, University of Heidelberg, Germany.

Scharr, H., and Weickert, J. (2000). An Anisotropic Diffusion Algorithm with Optimized Rotation Invariance. In: Proceedings of 22th DAGM-Symposium, Kiel, Germany, 460–467. DOI: 10.1007/978-3-642-59802-9.

Shokin, Y., Winnicki, I., Jasinski, J. et al. (2020a). High order modified differential equation of the Beam-Warming method. Part I: The dispersive features. Russ. *J. Numer. Anal. Math. Model.*, 35(2), 83–94. DOI: 10.1515/rnam-2020-0007.

Shokin, Y., Winnicki, I., Jasinski, J. et al. (2020b). High order modified differential equation of the Beam-Warming method. Part II: The dissipative features. *Russ. J. Numer. Anal. Math. Model.*, 35(3), 175–185. DOI: 10.1515/rnam-2020-0014.

Shuman, G.F. (1956). *The computational difficulties fundamental to the balance equation.* Technical Memorandum of the Joint Numerical Weather Prediction Unit, 3(6).

Stateczny, A., and Nowakowski, M. (2006). Analytical radar image compression methods for comparative navigation. *Scientific Journals of the Maritime University of Szczecin*, 8, 93–101.

Stateczny, A., Kazimierski, W., Kulpa, K. (2020). Radar and sonar imaging and processing. *Remote Sens.*, 12(11). DOI: 10.3390/rs12111811.

Stateczny, A., Kazimierski, W., Kulpa, K. (2021). Radar and sonar imaging and processing (2nd edition). *Remote Sens.*, 13(22). DOI: 10.3390/rs13224656.

Strang, G., and Fix, G. (2008). An Analysis of the Finite Element Method. New Edition, 2nd edn. *Wellesley–Cambridge Press*.

Strikwerda, J.C. (2004). *Finite Difference Schemes and Partial Differential Equations*. Philadelphia: SIAM.

Tadeusiewicz, R., and Korohoda, P. (1997). Computer Analysis and Image Processing (in Polish). Progress of Telecommunication Foundation Publishing House, Krakow (1997). Retrieved from http://winntbg.bg.agh.edu.pl/skrypty2/0098/.

Thompson, P.D. (1955a). *Reduction of truncation errors in the computation of geostrophic advection and other Jacobians*. Technical Memorandum of the Joint Numerical Weather Prediction Unit, 1(12).

Thompson, P.D. (1955b). *Reduction of truncation errors in the computation of geostrophic vorticity, the Laplacian operator, and its inverse*. Technical Memorandum of the Joint Numerical Weather Prediction Unit, 2(9).

Torre, V., and Poggio, T. (1984). On edge-detection. *IEEE Trans. Pattern Anal. Machine Intelligen.*, 8, 147–163. DOI: 10.1109/TPAMI.1986.4767769.

Warming, R.F., and Hyett, B.J. (1974). The modified equation approach to the stability and accuracy of finite difference methods. *J. Comp. Phys.*, 14(2), 159–179. DOI: 10.1016/0021-9991(74)90011-4.

Winnicki, I., Jasinski, J., Pietrek, S. (2019). New approach to the Lax–Wendroff modified differential equation for linear and non-linear advection. *Numer. Methods Partial Differ. Equ.*, 35(6), 2275–2304. DOI: 10.1002/num.22412.

Winnicki, I., Pietrek, S., Jasinski, J. et al. (2022). The mathematical characteristic of the Laplace contour filters used in digital image processing. The third order filters. *Adv. Geod. Geoinf.*, 71(2), article no. e23. DOI: 10.24425/gac.2022.141176.

Wojtkowska, M., Kedzierski, M., Delis, P. (2021). Validation of terrestrial laser scanning and artificial intelligence for measuring deformations of cultural heritage structures. *Measurement*, 167. DOI: 10.1016/j.measurement.2020.108291.